

## Band signatures in the low-energy-electron reflectance spectra of fcc metals

R. C. Jaklevic and L. C. Davis

*Engineering and Research Staff, Ford Motor Company, Dearborn, Michigan 48121-2053*

(Received 13 July 1982)

The elastic reflectance spectra for low-energy electrons (0–30 eV) of fcc metals show characteristic structure related to critical points in the energy bands. The (111) surfaces of Au, Ag, Pd, Cu, Ni, and Al have been investigated and all have spectra consisting of a sharp reflectance peak followed by a broad, more intense peak at higher energy. The broad peak correlates with the forbidden gap formed by the (222) Bragg reflection. The sharp peak is insensitive to the angle of incidence and lies very near the  $\Gamma'_2$  ( $\Gamma'_{25}$  in Al) energy. From a pseudopotential model we demonstrate the connection between the spectra and the band structure. Good quantitative agreement of the peak positions with previous band calculations and photoemission data is obtained and the behavior with angle is understood qualitatively. Ultrathin metals (a few atomic layers) and thick films deposited on single-crystal or amorphous substrates produce similar reflectance spectra. This technique can be applied to the study of metal surfaces and to the initial growth stages of epitaxial films.

### I. INTRODUCTION

Electron reflection has been used in a variety of ways to probe electronic states and atomic arrangements in the surface region of solids. For example, low-energy electron diffraction (LEED) is concerned with energy values at or above the threshold for external diffracted beams.<sup>1</sup> The study of surface resonances in the region just below threshold has been useful for understanding the surface-barrier potential.<sup>2</sup> A forbidden energy gap in Cu near the vacuum level<sup>3</sup> and free-electron standing wave states in Au films<sup>4</sup> have been previously observed by electron reflectance techniques. We report the observation of structure in the reflectance spectra of metals which not only is characteristic of the surfaces studied, but also can be understood by direct comparison with the electronic band structure of the metal.

Our results show the following: (a) The reflectance spectra obtained from (111) surfaces of all fcc metals studied (Au, Ag, Pd, Cu, Ni, Al) show intense characteristic elastic structure well below the threshold for the first nonspecular LEED beam. This structure is in the form of a sharp peak at the low-energy side of a more intense broad peak. (b) The broad peak correlates with the band gap formed by the (222) Bragg reflection. The sharp one occurs in a small angular range about normal incidence with a peak energy nearly independent of angle. It correlates with the energy band states  $\Gamma'_2$  ( $\Gamma'_7$  in double group notation) as determined by

band calculations and by final-state resonances in photoemission experiments. (c) Model calculations provide a basis for this interpretation and show that the sharp structure results from the crossing of two  $\Lambda_1$  bands, the free-electron-like band from  $\Gamma_{15}$  to  $L_1$  and the nearly flat band extending from  $\Gamma'_2$ . The theory also accounts qualitatively for the observed angle dependence. (d) Very thin layers of metal atoms, of the order of three to six atom layers, are sufficient to produce this structure. Even when deposited on amorphous substrates such layers produce similar results.

The electron reflectance measurements consist of directing a focused beam of electrons of variable energy at the target and measuring the collected current  $I_c$  in the target circuit.<sup>3</sup> Essentially, all electrons reflected by the target are collected by other electrodes in the chamber. Because the features of interest appear in both the reflected current  $I_R$  and the current collected by the sample  $I_c$ , the latter quantity is sufficient to determine the total reflective properties of the target. In Sec. II the experimental arrangement and details are described. Results for single crystals are presented in Sec. III A and compared to model calculations in Sec. III B. Section IV contains the results for thin films. Our concluding discussion is given in Sec. V.

### II. EXPERIMENTAL

The experiment is carried out in an ultrahigh vacuum chamber, ion pumped, bakable, and equipped

with a liquid-nitrogen-cooled titanium sublimation pump. The single-crystal metal surfaces are put through multiple cleaning cycles of argon-ion bombardment while heating to temperatures above their annealing point followed by vacuum annealing. The surfaces show normal LEED patterns over their entire area (12-mm diameter) which remain stable for many hours. These cleaning cycles are continued until stable and reproducible reflectance spectra are obtained from all areas of the metal surface. For other experiments, thin overlay films are formed by evaporating Au from a resistively heated source positioned near the substrate. Owing to difficulties in calibrating the quartz-crystal microbalance in this thickness range, film thicknesses could not be determined accurately to better than 50% for thicknesses less than about 25 Å. All of the structure reported here disappears with contamination of the surfaces.

The electron gun is a three-electrode type used for LEED applications and produces a current of 1  $\mu$ A. Use of a fluorescent screen target showed that the beam is focused to an area of 4 mm<sup>2</sup> or less with a maximum beam angle of 3° or less. The target manipulator is also equipped with a Faraday collector to measure incident beam current  $I_0$ . The second derivative  $I_c''$  was produced electronically by introducing a small ac modulation on the gun potential and detecting the second-harmonic com-

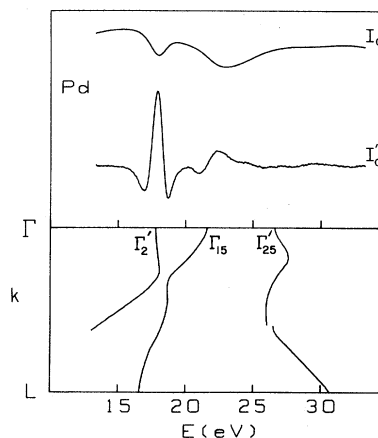


FIG. 1. Experimental plot of collected current  $I_c$  vs electron energy (referred to the Fermi energy of the target metal) for a Pd(111) surface at normal incidence and room temperature. The downward peaks in  $I_c$  correspond to elastic reflectance peaks. These become upward peaks in the second derivative spectrum  $I_c''$ . That portion of the band structure (see Ref. 5) important for determining the reflectance is also shown. The sharp downward peak at 17.9 eV corresponds to a 15% decrease in  $I$  referred to the current collected just below this energy where the bands are free-electron-like.

ponent of  $I_c$ . A second Faraday collector was mounted to measure the specular reflected beam at 5° from the normal-incidence angle. With this it was determined that all of the structure in the tar-

TABLE I. Comparison of energy ( $E - E_F$  in eV) of the peak in  $I_c''$  to  $\Gamma_2'(\Gamma_7^-)$  energy from band calculations and photoemission experiments. The intensities listed are for the percentage decrease of  $I_c$  for the smaller peaks referred to the current collected just below this energy where the bands are free-electron-like.

Metal	$I_c''$	Band calc.	Ultraviolet photoelectron spectroscopy	Intensity (%)
Au <sup>a</sup>	15.9,16.7	15.6 <sup>d</sup>	16.4 <sup>e</sup>	25
Pt <sup>b</sup>	16.5		16.6 <sup>e</sup>	
Ag	17.1	16.8 <sup>f</sup>	~16.5 <sup>g</sup>	13
Pd	17.9	17.7 <sup>h</sup>	18.4±0.5 <sup>i</sup>	15
Cu	23.7	25.1,23.3 <sup>j</sup>		5
Ni	24.3	23.8 <sup>k</sup>		8
Al <sup>c</sup>	13.3			5

<sup>a</sup>Double peak.

<sup>b</sup>Film.

<sup>c</sup>The lowest energy for Al is  $\Gamma_{25}' = 12.7$  eV (see Ref. 6).

<sup>d</sup>Reference 7.

<sup>e</sup>Reference 11.

<sup>f</sup>Reference 8.

<sup>g</sup>Reference 12.

<sup>h</sup>Reference 5.

<sup>i</sup>Reference 13.

<sup>j</sup>Reference 9.

<sup>k</sup>Reference 10.

get current  $I_c$  is also present in the specular reflected beam. From these measurements the total transmittance  $I_c/I_0$  or reflectance  $I_R/I_0$  could be obtained. From calibrated data it was found that the total transmittance just below the energy of the sharp peaks (i.e., where the electron states in the metal are free-electron-like) is typically about 90% for a clean metal and considerably less (e.g., 50%) for a contaminated surface. Thus the intensities listed in Table I may be considered as referred to the total incident current. The energy scale is determined by using an effective work function of 2.8 eV for the thoria emitter. The limiting resolution is determined by the thermal spread of the source which is estimated to be about 0.3 eV total width. Usually the inelastic reflected current was not measured but separate biasing experiments showed that this component is small (a few percent for a clean surface), slowly varying with energy, and does not contain any of the details studied here related to the elastic part of the reflectance.

### III. RESULTS—SINGLE CRYSTALS

#### A. Experiment

In Fig. 1 the experimental results for Pd at room temperature are shown. The collected current  $I_c$  is plotted and, to enhance the sharp peak at 17.9 eV, the second derivative spectrum  $I_c''$  is displayed. Also shown is the related section of the Pd band structure.<sup>5</sup> The broad (222) Bragg peak corresponds to the gap above  $\Gamma_{15}(\Gamma_8^-)$  while the sharp peak correlates with the band crossing near  $\Gamma_2'$ . This will be discussed in more detail later. Figure 2 shows a series of spectra obtained from Au, Ag, Cu, Ni, and Al. Except for differences in peak position and intensity, all bear a close resemblance to one another. However, for Au, a doublet is observed instead of a single peak. For Al, the extra structure above 25 eV is due to surface resonances, which are easily identified by the strong dependence of their peak position upon angle of incidence. Table I contains a comparison of the observed position of the sharp peaks with values obtained from band calculations<sup>5-10</sup> and also from final-state resonances in photoemission data.<sup>11-13</sup> The agreement is clearly very good. We do not expect the peak to be exactly at the  $\Gamma_2'$  point since the band crossing, which we believe is responsible for this feature, may occur at a slightly different energy. The position and qualitative behavior of the band gap corresponding to the (222) Bragg reflection is also in good agreement with

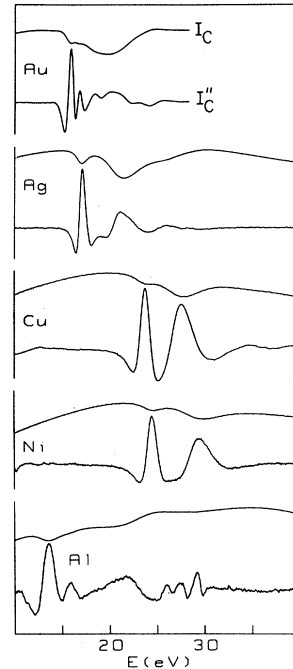


FIG. 2. Experimental plot of the collected current  $I_c$  (upper curve) and its second derivative  $I_c''$  (lower curve) vs electron energy (referred to the Fermi energy of the target metal) for (111) surfaces of some fcc metals. The extra structure above 25 eV for Al is due to surface resonances (see Ref. 2). The intensities listed in Table I establish the scale for each of the  $I_c$  plots.

known band structure. The variation of the spectra with the angle of incidence of the electron beam is shown in Fig. 3 for Cu and Au. For these the intensity of the sharp peaks drops to zero at 8° (Cu) and 12° (Au, 15.9-eV peak) with a slight downward shift (0.4 eV) for Cu, but no observable shift ( $< 0.1$  eV) for Au. This behavior is found for the other metals with some differences in both the angular extent as well as the observed shift of the peaks. At 600°C, the  $\Gamma_2'$  peaks for Au, Pd, and Cu were observed to be shifted upward by 0.15, 0.1, and 0.4 eV, respectively. However, the (222) broad peaks were shifted downward slightly. The downward shift agrees with expectations based on the thermal expansion of the lattice.

#### B. Model calculations

To establish the relationship between the reflected electron current and the bulk band structure, we have calculated the electron reflectance for the (111) surface of an fcc metal. A simple model was used that resembles the band structure and pseudopotential

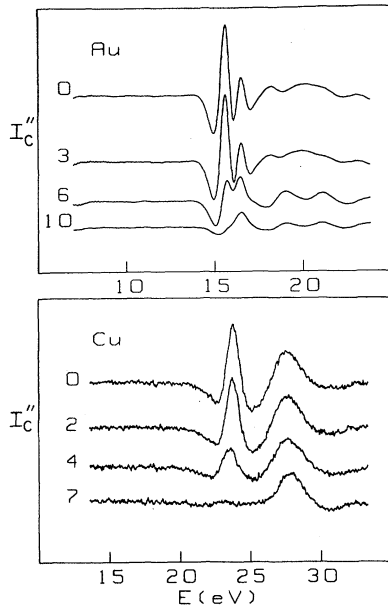


FIG. 3. Variation of reflectance peaks with angle of incidence of the electron beam for Cu and Au on an azimuthal plane passing through a [110] (for Cu) and [112] (for Au) direction on the surface. Note the small downward shift for Cu by about 0.4 eV at 8° and the absence of a shift for Au.

tial approaches to LEED,<sup>1,14</sup> rather than multiple-scattering formalisms that emphasize geometrical effects.<sup>1,15</sup> We approximate the crystal potential by

$$V(\vec{r}) = \sum_{\vec{G}} V_{\vec{G}} e^{i\vec{G} \cdot \vec{r}},$$

retaining the same Fourier coefficients as Smith<sup>16</sup> did for the plane-wave portion of his combined interpolation scheme. At the midplane between two layers, the bulk potential is terminated and replaced by a truncated image potential<sup>17</sup> to represent the vacuum region. Inelastic scattering (absorption) is described by an imaginary potential  $-iV_{0i}$  in the crystal which drops abruptly to zero at the surface.

For normal incidence, the wave function is expanded as

$$\psi(\vec{r}) = \sum_{\vec{g}} \psi_{\vec{g}}(z) e^{i\vec{g} \cdot \vec{r}},$$

where  $\vec{g}$  is a reciprocal net vector and  $z$  is perpendicular to the surface. Inside the crystal, the  $\psi_{\vec{g}}(z)$  are determined numerically; outside, they are approximated by their WKB forms.  $\psi_0(z)$  represents an incoming and a reflected wave, whereas  $\psi_{\vec{g}}(z), \vec{g} \neq 0$ , decays away from the surface since the energies of interest are below the (10) beam threshold.

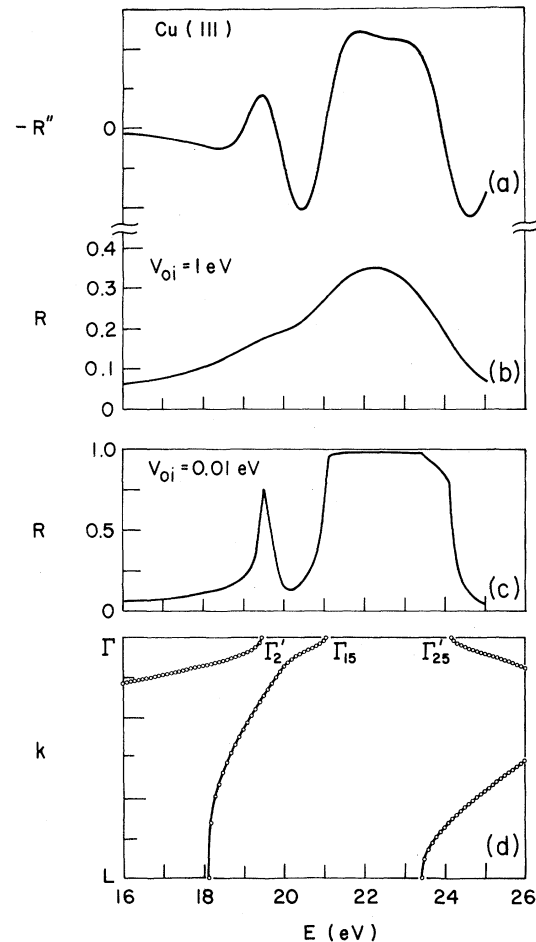


FIG. 4. Reflectance ( $R = I_R/I_0$ ) calculated from a pseudopotential model of Cu for two values of the absorption [(b) and (c)]. The energy  $E$  is relative to the vacuum level (not Fermi level). The negative second derivative ( $-R''$ ) has a peak within 0.1 eV of the  $\Gamma_2'$  energy (a). The  $\Lambda_1$  bands resulting from the model are shown for  $\vec{k}$  in the [111] direction (d).

In Fig. 4 we have plotted the reflectance  $R$  versus the incident electron energy  $E$  (relative to the vacuum level). The Fourier coefficients  $V_{\vec{G}}$  were chosen to give a reasonable description of the bands in the region of interest for Cu. Although the structure in the Cu reflectance is one of the weakest, we chose this metal for comparison because the bands are the most free-electron-like in this energy range and hence the easiest to describe.<sup>9</sup> For normal incidence only the  $\Lambda_1$  bands are required for matching at the interface and these are also shown in Fig. 4.

Considering first the results for negligible absorption ( $V_{0i} = 0.01$  eV) we see that a large gap exists between  $\Gamma_{15}$  and  $\Gamma_{25}$  that is due primarily to  $V_{222}$ ,

i.e., the Bragg reflection corresponding to  $\lambda=d_{111}$ . The reflection is  $\sim 100\%$  in this region because there are no states to which the incident wave can match. Below  $\Gamma_{15}$ , the free-electron band with wave function  $e^{i(\vec{k}-\vec{G}_{111})\cdot\vec{r}}$  easily transmits current except where it attempts to cross a rather flat band near  $\Gamma'_2$ . The wave function for the latter is made up of plane waves such as  $e^{i(\vec{k}-\vec{G}_{11-1})\cdot\vec{r}}$  which do not connect to propagating waves in the vacuum. Consequently, the reflection rises sharply at this energy. When absorption is included ( $V_{0i}=1$  eV), the reflectance is considerably smoother. However, the second derivative ( $-R''=d^2I_c/dE^2$  for unit incident current) displays a peak very close to the  $\Gamma'_2$  energy. Broader structure due to Bragg reflection is also present between  $\Gamma_{15}$  and  $\Gamma'_{25}$ .

The near constancy of the peak energy as a function of incident angle, particularly in the higher  $Z$  metals (such as Ag and Au), can be attributed to the flatness of the band near  $\Gamma'_2$ . Measurements of the angular region over which the peak persists correlates with the extent of the flat portion of the band in the direction perpendicular to  $[111]$ , e.g.,  $[1\bar{1}0]$ . We note that the sharpness of the peak implies that the absorption  $V_{0i}$  is small near the  $\Gamma'_2$  energy. The existence of a double peak in Au (0.8-eV splitting) may be associated with the small ( $\sim 4\%$ ) contraction of the surface along  $[1\bar{1}0]$ .<sup>18</sup> We saw evidence for this reconstruction in the LEED pattern in which the extra diffraction beams are grouped closely around the normal diffracted beams. Photoemission experiments<sup>11</sup> reveal a resonance corresponding to the higher, but weaker peak of the doublet in  $I_c''$ , as well as a possible resonance an electron volt or more lower. The upward shift of the sharp peak with increasing temperature probably requires a more detailed band calculation.

#### IV. THIN FILMS

Experiments were performed in which the targets consisted of crystalline and noncrystalline conducting substrates on which very thin layers of Au atoms were deposited. An example of the former is shown in Fig. 5(a) in which a series of spectra for increasing Au thickness on a Pd(111) surface are presented. The spectra are stable with time at room temperature and show no signs of alloying for temperatures below about 300°C. The Au-covered surface produces the same LEED pattern as a bulk Au(111) single crystal. Of interest is the fact that only a few atomic layers (2.3 Å per layer) of Au are required to transform the spectrum from Pd to that

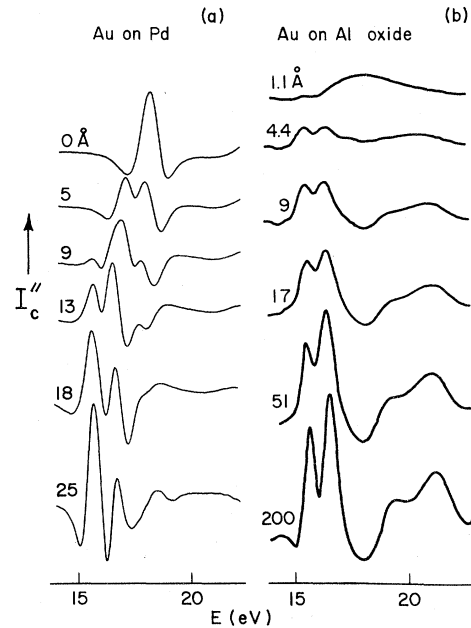


FIG. 5. Experimental plots of the second derivative of the collected current  $I_c$  vs electron energy (referred to the Fermi energy of the target) for Au deposited on a single-crystal Pd target (a) and an oxidized Al target (b). The thicknesses shown are accurate to about 50% for values below about 25 Å. The Al is a film of about 1000-Å thickness oxidized by exposure to pure oxygen at 1-Torr pressure. The intensity of the bottom spectrum of (a) is the same as listed in Table I for single-crystal Au. The scale for (b) is approximately one-fifth that of (a).

which is characteristic of Au. Three layers are required to completely cover a (111) fcc surface, as viewed from the normal direction. We note that as the Au is deposited the Pd peak is gradually reduced and replaced by the two Au peaks, first the one at 16.7 eV and then the one at 15.9 eV. As mentioned above, the absolute thickness calibration is no better than about 50% uncertainty but it is clear that the Au bands are formed near their bulk values as the first few monolayers are formed, and develop into a spectrum of full intensity when about ten layers are present. This corresponds to about one electron mean free path at this energy. A description of this behavior is beyond the scope of the present model. Similar results are found for Cu and Ag crystal substrates. For Au on Ag, it is known from Rutherford backscattering<sup>19</sup> that the Au atoms cover the Ag in a layer-by-layer sequence. The evidence here supports this mechanism for Pd and Cu substrates as well.

Results for Au on oxidized Al, a noncrystalline substrate, are shown in Fig. 5(b). The characteristic Au reflectance peaks begin to appear at about one-

half monolayer and persist to hundreds of layers or more. This behavior is repeated for Au-deposited other conducting substrates, e.g., amorphous carbon and oxidized Ni. The rate of growth of the signal with thickness varies somewhat with the nature of the substrate which indicates that the surfaces are not covered in a layer-by-layer mode noted above. These films are polycrystalline and the spectra obtained from them are somewhat different in detail from single-crystal data. However, it is common for films to be aligned preferentially with their close-packed direction [111] perpendicular to the surface. The degree of alignment of individual microcrystals is sufficiently good that peaks almost identical to the single-crystal reflectance are seen. We have examined all of the metals shown in Fig. 2 in thin-film form and all produce identifiable reflectance structure due to the band effects discussed. Usually, the reflectance peaks are weaker and depend on the type and roughness of the substrate. The relative insensitivity of the energy of the sharp peaks with angle (Fig. 3) explains the persistence of these features for polycrystalline thin films. Previous reports of structure in electron reflectance spectra for thin films<sup>20,21</sup> can also be understood in light of these and the single-crystal data.

Preliminary results with Pt and Ir films also reveal this structure. Data from Pt are listed in Table I and good agreement of the peak position with photoemission results is obtained. It is anticipated that spectra resembling those already reported will be found for single-crystal surfaces of these metals. In both cases it appears that the peaks are doublets, as in the case of Au, a result consistent with the known tendency of these three metals to form reconstructed surfaces.<sup>22</sup>

## V. DISCUSSION

There is reason to expect that these types of measurements should be applicable to other metals, other crystal faces, and semiconductors as well. Initial experiments on the Au(100) face have not been successful because of the number of diffracted-beam thresholds in this energy range produced by the

reconstruction of this surface. Further complications are expected for those metals where extra structure due to surface resonances appear (see Fig. 2 for Al). For (111) surfaces, the band structure of interest is typically at about half the threshold energy for diffracted beams, so interference from surface resonances is not a problem. In fact, no resonances just below the (10) beam threshold were detected in any metal except Al. This may indicate that disorder and/or impurities at the surface are far less important for the band-structure effects studied here than for surface resonances. More experiments are needed to establish the limits of applicability of this experimental approach.

We have shown that it is possible to directly measure the position of certain critical points in the band states of metal targets by measurement of electron reflection. The method is relatively simple, comprised of a standard electron gun and electronic components and may be used in conjunction with other measurements. It can be applied to other metal or semiconductor surfaces and also to layered or composite materials. This data is in the same energy range accessible to photoemission and optical absorption experiments, so the data are complementary. Because the electron reflection is sensitive only to the outermost few atomic layers, the development of band-structure details during growth can be studied. We are surprised that, with the first few layers of growth, the sharp peak has assumed the bulk value to within a few tenths of 1 eV.

From a more practical viewpoint, the method can be useful for the identification and analysis of layer-by-layer growth of epitaxy films or layered device structures. Very small deposits, such as dispersed supported metal catalysts can also be detected.

## ACKNOWLEDGMENT

We thank Dr. N. V. Smith for providing us with a copy of his band-structure program. We also gratefully acknowledge the technical assistance of Mr. L. Elie.

<sup>1</sup>J. B. Pendry, *Low-Energy Electron Diffraction* (Academic, London, 1974); M. A. Van Hove and S. Y. Tong, *Surface Crystallography by LEED* (Springer, Berlin, 1979).

<sup>2</sup>E. G. McRae, *Rev. Mod. Phys.* **51**, 541 (1979) and

references contained therein.

<sup>3</sup>E. G. McRae and C. W. Caldwell, *Surf. Sci.* **57**, 77 (1976).

<sup>4</sup>R. E. Thomas, *J. Appl. Phys.* **41**, 5330 (1970).

<sup>5</sup>N. E. Christensen, *Phys. Rev. B* **14**, 3446 (1976).

- <sup>6</sup>F. Szmulowicz and B. Segall, Phys. Rev. B 21, 5628 (1980).
- <sup>7</sup>N. E. Christensen, Phys. Rev. B 13, 2698 (1976).
- <sup>8</sup>N. E. Christensen, Phys. Status Solidi B 54, 551 (1972).
- <sup>9</sup>G. A. Burdick, Phys. Rev. 129, 138 (1963); J. F. Janak, A. R. Williams, and V. L. Moruzzi, Phys. Rev. B 11, 1522 (1975).
- <sup>10</sup>F. Szmulowicz and D. M. Pease, Phys. Rev. B 17, 3341 (1978).
- <sup>11</sup>K. A. Mills, R. F. Davis, S. D. Kevan, G. Thornton, and D. A. Shirley, Phys. Rev. B 22, 581 (1980).
- <sup>12</sup>P. S. Wehner, R. S. Williams, S. D. Kevan, D. Denley, and D. A. Shirley, Phys. Rev. B 19, 6164 (1979).
- <sup>13</sup>F. J. Himpsel and D. E. Eastman, Phys. Rev. B 18, 5236 (1978).
- <sup>14</sup>D. S. Boudreaux and V. Heine, Surf. Sci. 8, 426 (1967); G. Capart, *ibid.* 13, 361 (1969).
- <sup>15</sup>G. E. Laramore, Phys. Rev. B 9, 1204 (1974).
- <sup>16</sup>N. V. Smith, Phys. Rev. B 19, 5019 (1979); R. Lässer, N. V. Smith, and R. L. Benbow, *ibid.* 24, 1895 (1981). We used  $V_{000} = -0.80848$ ,  $V_{111} = 0.11392$ ,  $V_{200} = 0.085$ ,  $V_{220} = 0.0466$ ,  $V_{311} = 0.02856$ , and  $V_{222} = 0.1808 Ry$ .
- <sup>17</sup>R. E. Dietz, E. G. McRae, and R. L. Campbell, Phys. Rev. Lett. 45, 1280 (1980). We took  $U(0) = -5 eV$  and  $z_0 = -4 a.u.$
- <sup>18</sup>Y. Tanishiro, H. Kanamori, K. Takayanagi, K. Yagi, and G. Honjo, Surf. Sci. 111, 395 (1981) and references contained therein.
- <sup>19</sup>R. J. Culbertson, L. C. Feldman, P. J. Silverman, and H. Boehm, Phys. Rev. Lett. 47, 657 (1981).
- <sup>20</sup>R. C. Jaklevic, Bull. Am. Phys. Soc. Ser. II 26, 395 (1981).
- <sup>21</sup>S. A. Komolov and L. T. Chadderton, Surf. Interface Anal. 1, 82 (1979).
- <sup>22</sup>P. Heimann, J. Hermanson, H. Miosga, and H. Neddermeyer, Phys. Rev. Lett. 43, 1757 (1979).